HOSTED BY

ELSEVIER

CrossMark

Available online at www.sciencedirect.com

ScienceDirect

Journal of Magnesium and Alloys 2 (2014) 230–238
www.elsevier.com/journals/journal-of-magnesium-and-alloys/2213-9567

Full length article

Effect of Ca addition on modification of primary Mg_2Si, hardness and wear behavior in Mg–Si hypereutectic alloys

M.E. Moussa [a,*], M.A. Waly [a], A.M. El-Sheikh [b]

[a] *Department of Manufacturing Technology, Laboratory of Foundry, Central Metallurgical Research and Development Institute (CMRDI), P.O. 87, Halwan, Egypt*
[b] *Department of Mining, Petroleum and Metallurgical Engineering, Faculty of Engineering, Cairo University, P.O. 12613, Giza, Egypt*

Received 3 June 2014; accepted 25 September 2014
Available online 4 November 2014

Abstract

The effect of Ca addition on modification of primary Mg_2Si, hardness and wear behavior in Mg–5 wt.%Si hypereutectic alloy has been investigated. The results showed clearly that without Ca addition, most of primary Mg_2Si appeared as coarse dendritic morphology with average size of about 215 μm. With the addition of 0.1 wt.%Ca, the average size of primary Mg_2Si decreased to about 98 μm, but their morphologies did not significantly changed. As the addition level of Ca increased to 0.3 wt.%, the average size of primary Mg_2Si decreased significantly to about 50 μm and their morphologies changed to polyhedral shape. However, with further increasing Ca addition to 0.6 wt.% and 1 wt.%, some needle-like and blocky CaMgSi particles formed and the average size of primary Mg_2Si increased slightly, which could described as over-modification. The present work showed that the optimal modification effect could be obtained when the Ca content in the investigated alloy reached 0.3 wt.%. The modification mechanism may be referred mainly due to poisoning effect resulting from the segregation of Ca atoms at the growth front of the Mg_2Si and the adsorption effect of some Ca atoms in the Mg_2Si crystal growth plane. The 0.3 wt.%Ca-added alloy has the highest hardness value and the best wear resistance among all other alloys. An excessive Ca addition resulted in the formation of some needle-like and blocky CaMgSi particles, which was detrimental to hardness and wear behavior of the 0.6 wt.% and 1 wt.%Ca-added alloys. The wear mechanism of investigated alloys is a mild abrasive oxidative wear with little adhesion.

Keywords: Mg–Si alloys; Modification; Ca addition; Hardness; Wear

1. Introduction

Lightweight magnesium alloys have attracted significant interest in the last decade due to their potential applications in automotive, electronics and aerospace industries [1–4]. Meanwhile, improving the elevated temperature properties has become a critical issue for possible application of magnesium alloys in hot components [5,6].

In recent years, the fascinating properties and promising application of hypereutectic Mg–Si alloys have attracted particular interest due to the formation of thermally stable Mg_2Si phase [7–9]. It is known that the intermetallic compound of Mg_2Si exhibits an excellent combination of superior properties, such as high melting temperature (1085 °C), low density (1.99×10^3 kg m^{-3}), high hardness (4.5×10^9 Nm^{-2}), low thermal expansion coefficient (7.5×10^{-6} K^{-1}) and reasonably high elastic modulus (120 GPa), which greatly improve the heat-resistance and wear resistance of the hypereutectic Mg–Si alloys [10–13]. However, the hypereutectic Mg–Si alloys prepared by ordinary ingot metallurgy process showed very low ductility and strength due to the large primary Mg_2Si particle size and the brittle eutectic phase [11–13].

* Corresponding author. Tel./fax: +20 2 25010095.
E-mail addresses: eissa83@yahoo.com, m_eissa83@yahoo.com (M.E. Moussa).
Peer review under responsibility of National Engineering Research Center for Magnesium Alloys of China, Chongqing University.

http://dx.doi.org/10.1016/j.jma.2014.09.005.

Various researches are aimed at improving the mechanical properties of Mg_2Si reinforced Mg-alloys through processes, such as strain induced melt activation process [10], hot extrusion [14], rapid solidification [15] and mechanical alloying [16]. However, compared with the above-mentioned techniques, modification treatment is a more cost-effective processing technique and available for generally commercial application.

Our recent research [11] has shown that the primary Mg_2Si could be effectively refined and modified by the application of high intensity ultrasonic treatment on the hypereutectic Mg−5 wt.%Si alloy during solidification process. It has been reported that Y [13], KBF_4 [17,18], La [19] and Y_2O_3 [20] can refine the primary Mg_2Si in Mg−Si alloys. Surface active elements such as Sr, Ca, P, Ba and Bi have been added to Si-containing Mg alloys to modify the morphology of Mg_2Si [21−28]. Among them, Ca could modify and refine both the primary and eutectic Mg_2Si in Mg−6Zn−4Si alloy [23] as well as eutectic Mg_2Si in Mg−6Zn−1Si [24] and Mg−5Al−1Zn−1Si alloy [25]. However, up to now, the modification effect of Ca on microstructure and wear behavior of hypereutectic Mg−Si alloys has not been reported. Therefore, The main aims of this work are to investigate the effect of Ca addition on modification of primary Mg_2Si, hardness and wear behavior in Mg−5 wt.%Si hypereutectic alloy and to explore modification and wear mechanisms.

2. Experimental procedures

2.1. Materials and processing

Commercial pure Mg (99.8 wt.% purity) and Si (99.8 wt.% purity) were used as starting materials. Charge of about 15 kg with the nominal composition of hypereutectic Mg−5 wt.%Si alloy was prepared as the base material in the present study. The charge was melted in a graphite crucible by a 200 kW medium frequency induction furnace. The melting, remelting and casting processes were carried out under the mixed gas protection consists of tetrafluoroethane (CF_3CH_2F, HFC-134a, 1 vol.%) and carbon dioxide (CO_2, Bal.). Firstly commercial Mg ingots were melted to above 650 °C, and then silicon was added into Mg melt. After that the melt was heated to above 800 °C and kept about 30 min to ensure Mg and Si fully reacted and formed Mg_2Si. Finally the melt was poured into a cast iron mold. The hypereutectic Mg−5 wt.%Si alloy ingots were sliced for subsequent experiments.

The hypereutectic Mg−5 wt.%Si of about 1.5 kg was remelted in a mild steel crucible using an electric resistance furnace. Nominal amounts of Ca (0, 0.1 wt.%, 0.3 wt.%, 0.6 wt.% and 1 wt.%) in the form of high purity Ca (99.999 wt.%) were added into the remelted alloys at about 800 °C. The melt was manually stirred for 3 min using a stainless steel rod, and then was held for additional 15 min in order to get full homogenization. After that the slag was removed, and then the melt was poured at about 800 °C into a cylindrical resin−bonded sand mold with dimensions of outer diameter (Ø100 mm), inner diameter (Ø42 mm) and length (250 mm). The reason for using a cylindrical resin-bonded sand mold is to reduce the cooling rate effect on the resulted microstructures of the prepared samples. Therefore, the difference in the morphology and size of primary Mg_2Si in the microstructures of investigated samples were obtained mainly as a result of the difference in the amounts of Ca.

The solidification characteristic of the prepared alloys was confirmed using thermal analysis. The thermal analysis test sample was obtained by pouring the quantity of the melt at about 830 °C into standard Qiuk-Cup resin-bonded sand cup with dimensions described in Fig. 1. A high sensitivity type K thermocouple (chromel−alumel) located vertically at the center of the cup, facilitated the capturing of the temperature during solidification. The data for thermal analysis were collected using a data logger and transferred to a personal computer for analysis. Thermal analysis trial was repeated three times to ensure reproducibility of the results. The chemical compositions of the prepared alloys were measured with X-ray fluorescence (XRF) analyzer (model Axios advanced-PANALYTCAL, The Netherlands) as shown in Table 1.

2.2. Materials characterization

All metallographic specimens were cut at the same position of 10 mm from the bottom of castings. The samples were prepared according to usual procedures developed for

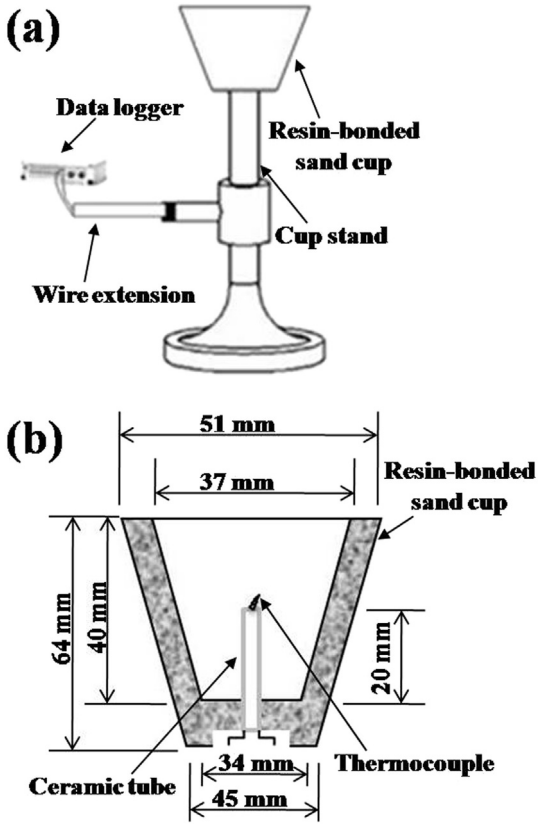

Fig. 1. Schematic of (a) experimental setup for thermal analysis and (b) resin-bonded sand cup with type K thermocouple.

Table 1
The chemical composition of the prepared alloys (wt.%).

Prepared alloy	Mg	Si	Ca	Fe	Cu
Mg–5Si	Bal.	5.02	–	0.033	0.041
Mg–5Si–0.1Ca	Bal.	5.085	0.109	0.031	0.045
Mg–5Si–0.3Ca	Bal.	5.059	0.342	0.031	0.043
Mg–5Si–0.6Ca	Bal.	5.012	0.598	0.031	0.042
Mg–5Si–1Ca	Bal.	4.966	0.902	0.032	0.036

magnesium alloys [29] and etched by solution with 10 ml nitric acid, 30 ml acetic acid, 40 ml water, and 120 ml ethanol for 2–3 min. The microstructures of the specimens were analyzed by optical microscope (OM) (model OPTIKA M-790, Italy). In the present study, the average length of primary Mg_2Si was measured as the size of Mg_2Si. Six OM micrographs were taken for each sample from the observed area at a low magnification of 100×. The average size of the primary Mg_2Si was measured by ImageJ1.44 software. All Mg_2Si existed in one picture taken from the observed area were measured.

Energy dispersion spectrum (EDS) affiliated to field emission scanning electron microscopy (FESEM) (model Quanta FEG, The Netherlands) was performed to reveal the concentration of alloying elements in selected areas of the microstructure. Phase constituents of samples were analyzed by X-ray diffraction (XRD) (model X'PERT PRO, The Netherlands) using Cu Kα radiation in step scan of 2θ from 20° to 120° with an increment of 0.02° and a scanning speed of 4°/min.

2.3. Hardness and wear tests

The Vickers hardness test of the prepared alloys using the metallographic specimens, at room temperature, was carried out in a Vickers hardness tester (model INSTRON WOLPERT GMBH–930/250, England) with a normal load of 3 kgf (designated as HV_3). The mean of ten successful measurements was taken to establish the hardness values.

Dry sliding wear tests without lubricant were conducted using a pin-on-disc type apparatus (model TNO TRIBOMETER, The Netherlands) in accordance to the ASTM G99-05 standard. The cylindrical pin specimens having diameter (Ø7 mm) and length (12 mm) machined out from the same position of the prepared castings were used as test samples. Hardened ball bearing steel disc (HRC 63) of outer diameter (Ø73 mm), inner diameter (Ø65 mm) and thickness (25 mm) was used as the counterpart surface. Specimens and counterpart surfaces were ground with different emery papers up to 1200 grit and cleaned ultrasonically in acetone to avoid the presence of humidity and non-desirable deposits. During testing, a jet of compressed air was pointed at the edge of the disc to avoid accumulation of wearing particles on the disc. All tests were performed under ambient atmosphere using a stationary load of 10 N and a constant sliding speed of 0.3 m/s for 10 min. The weights of the samples were measured before and after the experiment using electronic scales with 0.1 mg accuracy, after which the results of the experiment were evaluated according to the loss in weight. Worn surfaces and wear debris of the specimens were examined and analyzed using FESEM equipped with EDS in order to determine the post-experimental wear mechanisms.

3. Results

3.1. Material investigation

Fig. 2 shows the XRD results of the as-cast prepared alloys. As shown in Fig. 2, all the prepared alloys are mainly composed of Mg_2Si and Mg phases. However, the Ca-containing alloys with the addition of 0.6 wt.%Ca and 1 wt.%Ca, a new CaMgSi is found. The absence of the new CaMgSi in the alloys with the additions of 0.1 wt.%Ca and 0.3 wt.%Ca is presumably ascribed to the relatively small amount of Ca.

Fig. 3 shows the cooling curves with its first derivative curves of the as–cast prepared alloys. It is found from Fig. 3a that the primary Mg_2Si began to precipitate from the prepared alloy melt without Ca addition at about 767 °C as refereed to liquidus temperature (T_L). Then, along with the temperature decrease, the eutectic reaction occurs at about 633 °C (T_E). After adding Ca, the liquidus temperature is about 762 °C, 756 °C, 756 °C and 756 °C for the prepared alloys with 0.1 wt.%, 0.3 wt.%, 0.6 wt.% and 1 wt.%, respectively as shown in Fig. 3b–e. Also, the eutectic temperature is about 633 °C, 631 °C, 632 °C and 632 °C for the prepared Ca-added alloys with 0.1 wt.%, 0.3 wt.%, 0.6 wt.% and 1 wt.%, respectively. Therefore, addition of Ca has very obvious effect on decreasing the liquidus temperature of investigated Mg–5 wt.%Si hypereutectic alloy but slight effect on eutectic temperature of investigated alloy.

The optical images of the alloys with different Ca contents are shown in Fig. 4. Moreover, a relationship between Ca content and average size of primary Mg_2Si is shown in Fig. 5. The microstructures of hypereutectic base alloy reveal the presence of primary Mg_2Si, Mg halos and eutectic Mg–Mg_2Si. Moreover, all the primary Mg_2Si are surrounded

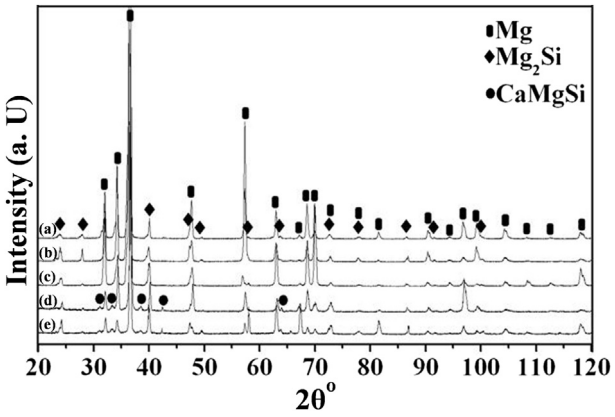

Fig. 2. XRD results of the as-cast Mg–5 wt.%Si alloy (a) without Ca addition and with Ca additions of (b) 0.1 wt.%, (c) 0.3 wt.%, (d) 0.6 wt.% and (e) 1 wt.%.

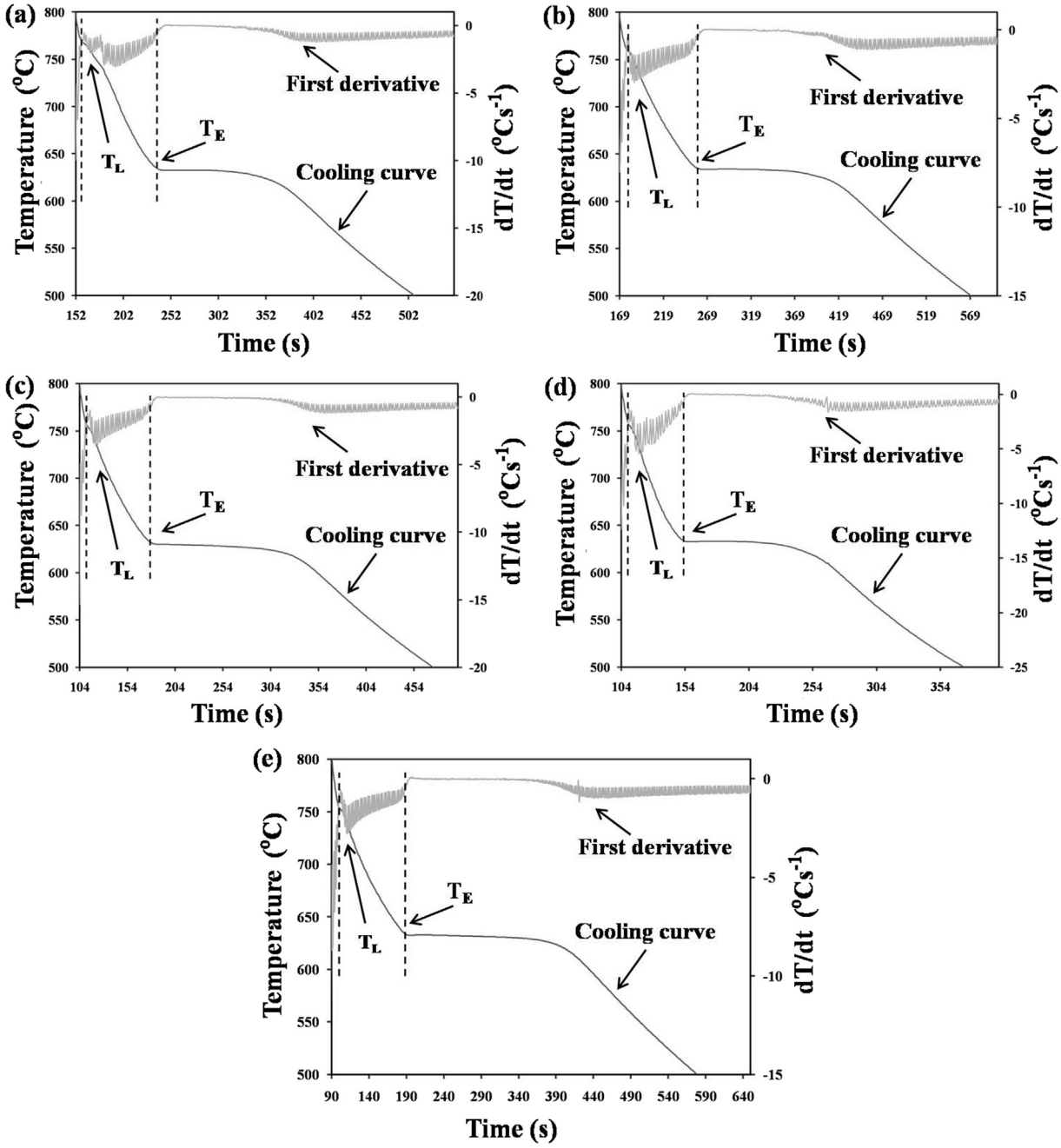

Fig. 3. The cooling curves with these first derivative curves of the as-cast Mg−5 wt.%Si alloy (a) without Ca addition and with Ca additions of (b) 0.1 wt.%, (c) 0.3 wt.%, (d) 0.6 wt.% and (e) 1 wt.%, where T_L (liquidus temperature) and T_E (eutectic temperature).

by Mg halos, and then by eutectic structure. Without Ca addition, most of primary Mg_2Si show coarse dendritic morphology (Fig. 4a) with the average size of about 215 μm (Fig. 5).

With 0.1 wt.%Ca addition, most of primary Mg_2Si are still dendrite (Fig. 4b), but their average size is reduced to about 98 μm (Fig. 5). When the Ca addition is increased to 0.3 wt.%, most of primary Mg_2Si become polyhedral shape (Fig. 4c) and their average size is significantly reduced to about 50 μm (Fig. 5). Fig. 6 shows the EDS line scan patterns of Mg, Ca and Si across a primary Mg_2Si and EDS elemental mapping of Mg, Si and Ca in the prepared Mg−5 wt.%Si−0.3 wt.%Ca alloy. It can be seen that a small enrichment of Ca is observed at the interface between the primary Mg_2Si and the matrix. Furthermore, some of Ca atoms could adsorb in Mg_2Si. However, when the Ca content is further increased to 0.6 wt.% and 1 wt.% (Fig. 4d and e), it is found that the average size of primary Mg_2Si is slightly increased again (Fig. 5) as means the appearance of over-modification. Moreover, some needle-like and blocky particles are formed due to an excessive Ca addition (Fig. 4d, e). Fig. 7 shows the EDS line scan patterns of Mg, Ca and Si across a needle-like and blocky particle and

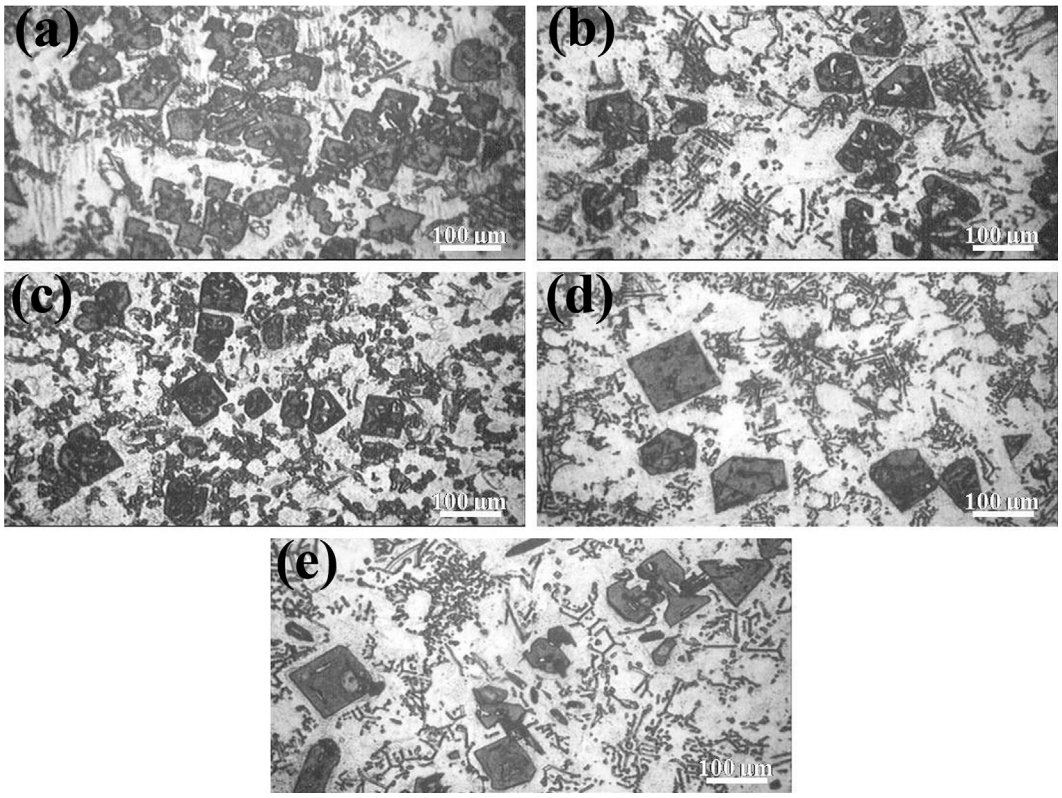

Fig. 4. Optical images of the as-cast Mg–5 wt.%Si alloys (a) without Ca addition and with Ca additions of (b) 0.1 wt.%, (c) 0.3 wt.%, (d) 0.6 wt.% and (e) 1 wt.%.

EDS elemental mapping of Mg, Si and Ca in the prepared Mg–5 wt.%Si–1 wt.%Ca alloy. The needle-like and blocky particle consists of Mg, Ca and Si. Combined with the XRD results shown in Fig. 2, it is found that the needle-like and blocky particle is most likely the CaMgSi particle. Therefore, the optimal modification effect is obtained when the Ca content in the investigated alloy is 0.3 wt.%.

3.2. Hardness and wear behavior

Fig. 8 demonstrates the average hardness values of the prepared alloys. It can be found that the average hardness value of the prepared alloys with Ca additions is higher than that of the alloy without Ca addition, implying that adding Ca element to the Mg–5 wt.%Si alloy can improve the hardness of the alloy. The average hardness values of the prepared alloys significantly increases with an increase in Ca content up to 0.3 wt.% and then gradually decreases with a further Ca addition. Therefore, the optimal hardness of the alloys can be achieved with Ca addition of 0.3 wt.% in this work.

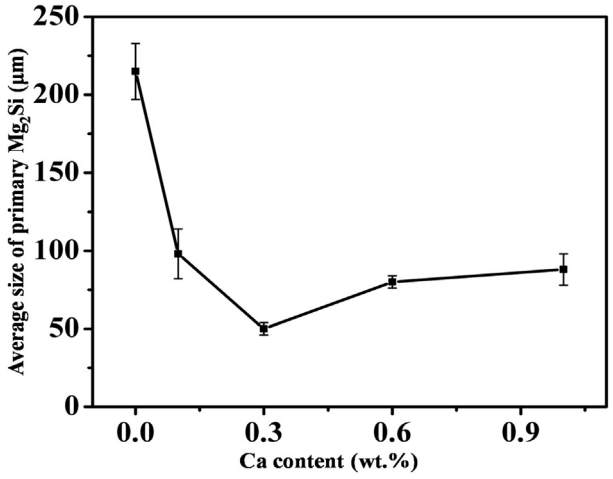

Fig. 5. The relationship between Ca content and average size of primary Mg_2Si.

Fig. 9 represents the weight loss of the prepared alloys. It can be found that the weight loss significantly decreases initially with an increase in Ca up to 0.3 wt.% and then gradually increases with a further Ca addition. This is basically coincident with the change trend in the average size of primary Mg_2Si of the prepared alloys. Therefore, the prepared alloy with addition of 0.3 wt.%Ca has the best wear resistance among all the other alloys due to the lowest weight loss.

Fig. 10 shows FESEM micrographs of the worn surfaces and their wear debris with their EDX analysis of investigated Mg–5 wt.%Si samples without Ca addition and with Ca additions of 0.3 wt.% and 1 wt.%. It is found that the worn surfaces after wear test exhibit different morphologies. Traces of parallel grooves and ridges can be observed on the surface of the sample without Ca addition (Fig. 10a) and 1 wt.%Ca-added sample (Fig. 10e). Furthermore, the surface of sample without Ca addition is rougher than that of the 1 wt.%Ca-added sample. The wear debris of sample without Ca addition and the 1 wt.%Ca-added sample are large size as shown in Fig. 10b and f which gives rise to a relatively high weight loss. The surface of the 0.3 wt.%Ca-added sample is relatively smooth surface as shown in Fig. 10c. The wear debris of the

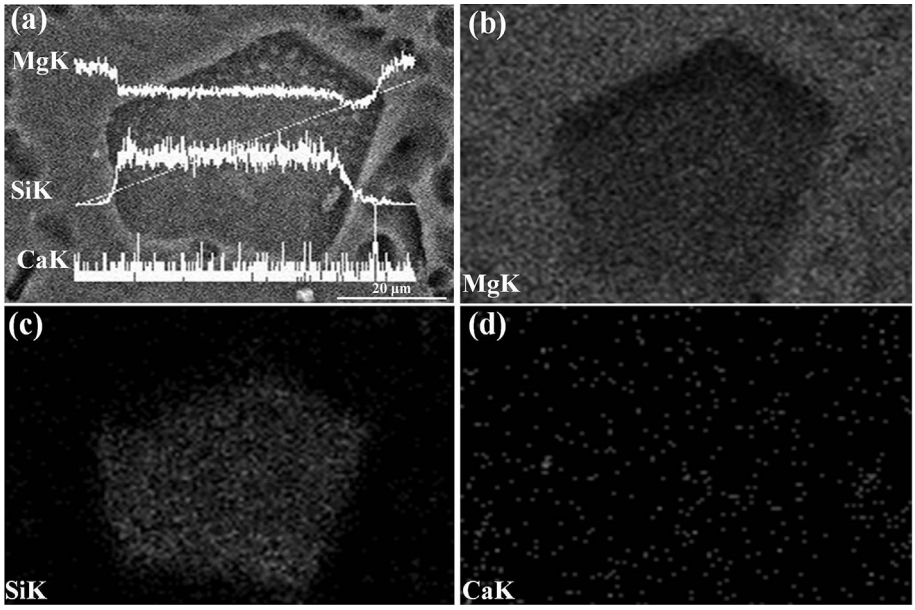

Fig. 6. (a) FESEM micrograph with the EDS line scan patterns of Mg, Ca and Si across a primary Mg_2Si and EDS elemental mapping of (b) Mg, (c) Si and (d) Ca in the prepared Mg–5 wt.%Si–0.3 wt.%Ca alloy.

0.3 wt.%Ca-added sample are also smaller in size as shown in Fig. 10d, which gives rise to a relatively low weight loss. For the Ca–added samples, analysis on the debris confirms the presence of Ca, besides Mg, Si, Fe and O (Fig. 10d and f) as compared with sample without Ca addition (Fig. 10b).

4. Discussion

4.1. Material investigation

Under the present experimental conditions, the effect of the cooling rate on the modification of primary Mg_2Si in hypereutectic Mg–5 wt.%Si could be negligible. Therefore, the difference in the morphology and size of primary Mg_2Si were resulted almost exclusively from the difference in the Ca addition. Usually, the microstructure of materials depends on the nucleation process and growth conditions [30]. For the Mg_2Si, its structure belongs to face centered cube (FCC) and its dendrite arm should grow along the preferential [100] crystallographic directions [18]. As a result, the morphologies of the primary Mg_2Si in the sample without Ca addition are mainly characterized by dendrites with complex morphologies, as shown in Fig. 4a.

In the present work, the morphology of the primary Mg_2Si changes obviously from dendritic (Fig. 4a) to polygonal particles with increasing Ca addition up to 0.3 wt.%Ca (Fig. 4c).

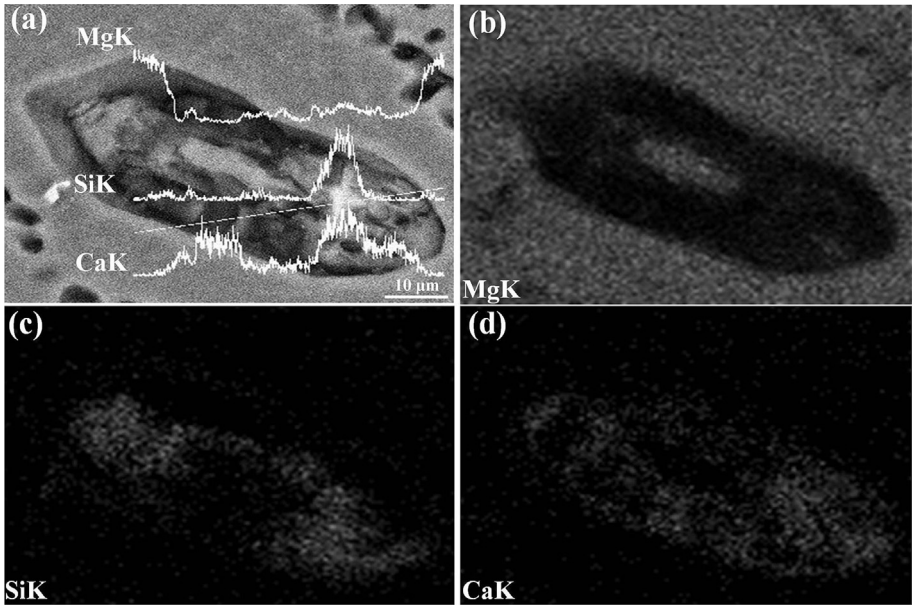

Fig. 7. (a) FESEM micrograph with the EDS line scan patterns of Mg, Ca and Si across a blocky CaMgSi phase and EDS elemental mapping of (b) Mg, (c) Si and (d) Ca in the prepared Mg–5 wt.%Si–1 wt.%Ca alloy.

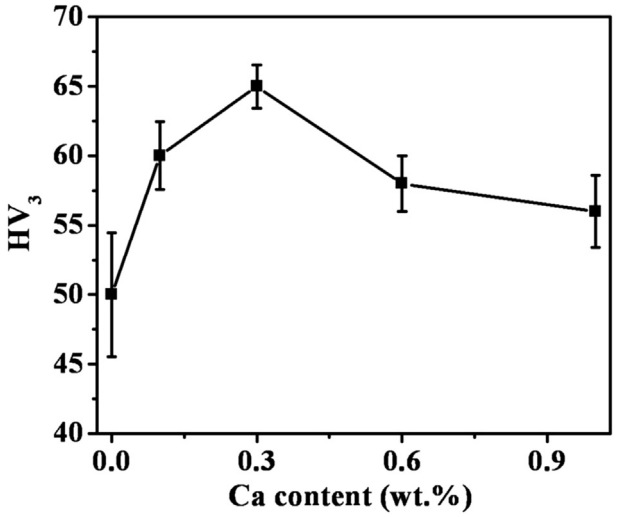

Fig. 8. Average hardness values of the prepared alloys.

According to the classic solidification theory, the relationship between the critical nucleus radius and the undercooling degree is given as follows [31]:

$$r^* = -\frac{2\sigma}{\Delta G_v} = \frac{2\sigma \cdot T_m}{L_m \cdot \Delta T} \quad (1)$$

where r^* is the critical nucleus radius, ΔG_v is the variation of volume free energy, σ is the interfacial energy of unit surface area, T_m is the equilibrium crystallizing temperature, L_m is the crystallizing latent heat and ΔT is the undercooling degree, which can be expressed as: $\Delta T = T_m - T$, where T is the onset crystallizing temperature.

Based on this equation, the critical nucleus radius could be reduced by increasing the undercooling degree or decreasing the interfacial energy, which would result in the decrease of the nucleation energy of the crystal nucleus and the increase of the probability of nucleation. Under the present experimental conditions, the liquidus temperature decreases from about 767 °C (Fig. 3a) of alloy without Ca addition to about 756 °C of alloy containing 0.3 wt.%Ca (Fig. 3c).Therefore, the Ca increases the undercooling degree, which would result in the increasing of effective number of the potential Mg_2Si crystal nucleus.

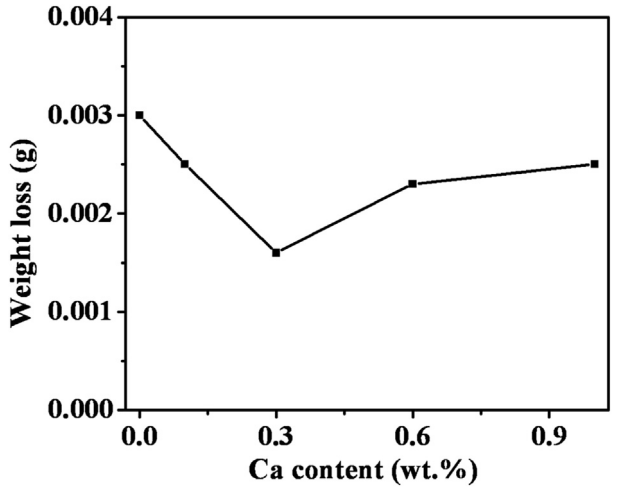

Fig. 9. Weight loss of the prepared alloys.

In addition to the increase of the probability of nucleation with 0.3 wt.%Ca, the segregation of Ca atoms at the liquid–solid interface as shown in Fig. 6a and d would restrict the Mg_2Si growth during solidification process. Furthermore, some of Ca atoms could adsorb in the Mg_2Si crystal plane as shown in Fig. 6a and d. It would reduce the surface energy of the Mg_2Si crystals by lattice distortion due to the existence of Ca in the Mg_2Si lattice, because the atomic radius of Ca with 2.23×10^{-10} m, is much larger than that of Mg or Si with 1.72×10^{-10} m, 1.46×10^{-10} m, respectively [23]. This results in the preferred growth habit and growth rate of the Mg_2Si phase being suppressed. Thus, all of these lead to the formation of polygonal type Mg_2Si. As such, the presence of Ca atoms on the growth front of the Mg_2Si caused a poisoning effect.

However, as the Ca content is increased to 0.6 wt.% and 1 wt.%, there exist some additional needle-like and blocky CaMgSi particles as shown in Fig. 4d and e. Under the equilibrium solidification conditions, CaMgSi particles can be crystallized from the molten alloy as the temperature decreases, and then the primary Mg_2Si is solidified [23]. Therefore, the formation of the CaMgSi particles resulted in the decrease in the volume fraction of the primary Mg_2Si, because a portion of the available Si is consumed previously. Meanwhile, the average size of primary Mg_2Si is slightly increased (Fig. 5) by the reduction of the effective Ca level as means the appearance of over-modification.

4.2. Hardness and wear behavior

It is well known that the fine microstructure is usually beneficial to the mechanical properties of engineering alloys [21]. In the present work, the coarse dendritic primary Mg_2Si in the Mg–5 wt.%Si alloy will give a detrimental effect on the hardness because of the tips of the primary Mg_2Si. Therefore, it can be inferred that the improvement of the hardness for the Mg–5 wt.%Si alloy modified by 0.3 wt.%Ca (Fig. 8) is possibly related to the modification and refinement of the hard primary Mg_2Si. However, the low hardness of the alloys with Ca additions of 0.6 wt.% or 1 wt.% is mainly attributed to the presence of needle-like CaMgSi particles. Therefore, a Ca content of 0.3 wt.% is beneficial to the hardness of the alloys in this work.

In the present work, the coarse dendritic primary Mg_2Si in the Mg–5 wt.%Si alloy without Ca addition will give a detrimental effect on its wear resistance because of the tips of the primary Mg_2Si. Furthermore, the high weight loss (Fig. 9), the surface scratches (Fig. 10a) and the large wear debris (Fig. 10b) of the sample without Ca addition may be attributed to coarse dendritic primary Mg_2Si detached from the contact face between pin and samples. The wear resistance of an alloy can generally be enhanced by introducing secondary phase(s) to the matrix material [32]. Nevertheless, microstructural

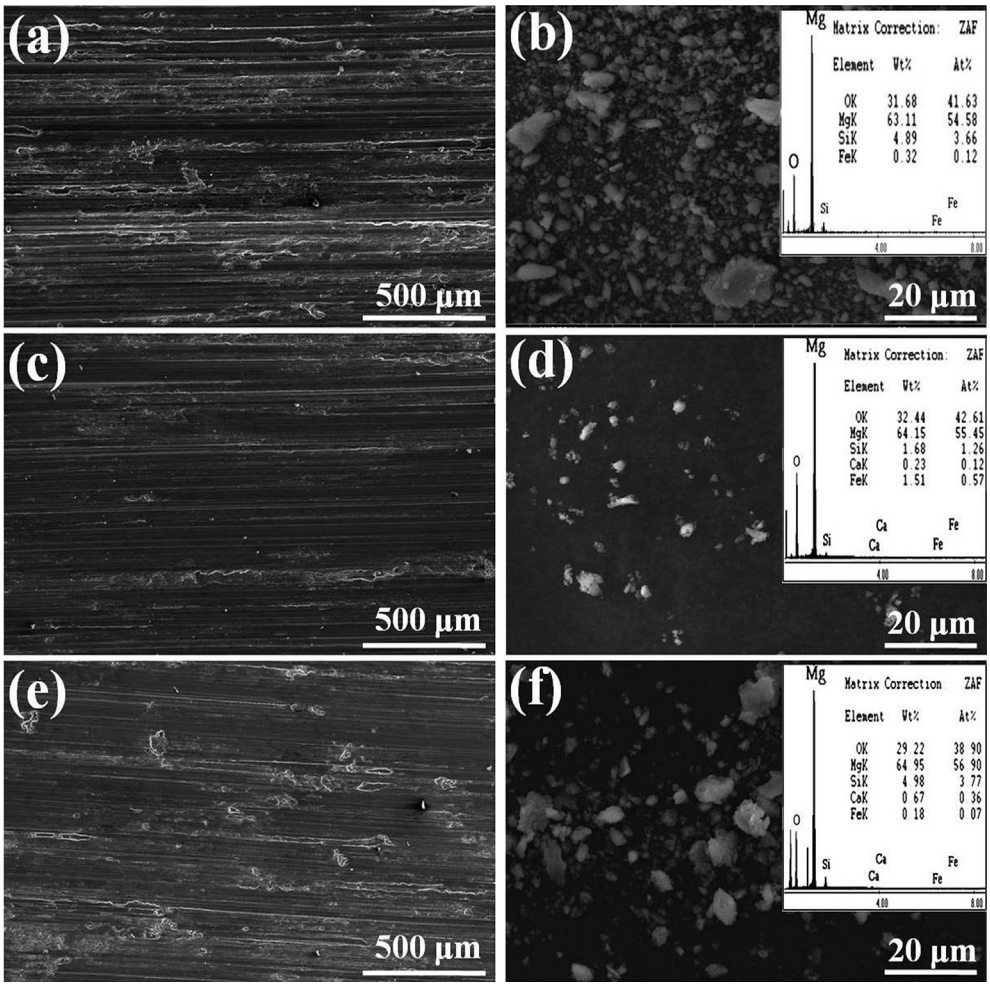

Fig. 10. FESEM micrographs of the worn surfaces and their wear debris with their EDX analysis of the investigated Mg−5 wt.%Si samples (a),(b) without Ca addition, and With Ca addition of (c),(d) 0.3 wt.% and (e),(f) 1 wt.%.

characteristics like morphology, size and distribution of hard particles have a great influence on the sliding wear properties of alloys [33]. In the present study, since the hard primary Mg_2Si is almost uniform distribution in the 0.3 wt.%Ca-added alloy, the abrasion degrees of contact face on the sample should be homogeneous. Furthermore, the fine Mg_2Si also reduces the extent of abrasion wear. Moreover, the 0.3 wt.% Ca-added alloy has the highest hardness value among other alloys which leads to the highest wear resistance. As cited in Ref. [3], the wear law states that the materials with higher hardness will exhibit better resistance to wear. Thus, all of these lead to the lowest weight loss (Fig. 9), the smooth surface (Fig. 10c) and the small wear debris (Fig. 10d) of the 0.3 wt.%Ca-added sample. Therefore, the best wear resistance of alloy is achieved with 0.3 wt.%Ca addition. However, the surface of Mg−5 wt.%Si alloy with 1 wt.%Ca addition is rough as shown in Fig. 10e. Besides the coarse Mg_2Si, it is also due to the presence of needle-like CaMgSi particles, which is arranged through sliding direction. The aculeate CaMgSi particles removed from the sample surfaces aggravate the abrasion wear, which is also responsible for the high weight loss (Fig. 9) and the large wear debris (Fig. 10f) of the 1 wt.%Ca-added alloy.

The presence of Fe in wear debris of investigated samples (Fig. 10b, d and f) is due to the plowing by hard primary Mg_2Si on the rotating steel disc [12,33]. Also, the presence of O was considered to have arisen in reactions with the environment, indicating that the mode of wear is mildly oxidative [33]. At very low loads an oxidative mechanism controls the wear process, generating debris comprising predominantly oxides. The oxidation was considered to take place due to the ability of the metal to oxidize under ambient conditions. On the other hand, material loss under abrasive wear conditions was removed by plowing and micro-cutting. These mechanisms required penetration by hard abrasive particles which in turn are controlled by the hardness of material [33].it has also reported [3] presence of abrasive wear in the low speed regime. Numerous grooves and shallow scratches running parallel to the sliding direction generally characterize abrasive wear [3]. In the present work, the wear test was carried out at a low sliding speed of 0.3 m/s under the applied load of 10 N which favor abrasive wear. The presence of grooves and ridges on the surfaces of the sample without Ca addition (Fig. 10a) and 1 wt.%Ca-added sample (Fig. 10e) characterize abrasive wear. Adhesion is a relevant wear mechanism in many lightweight alloys [34] and it was also observed in the wear

behavior of the AM50B Mg alloy [35]. The adhesion wear mechanism appears due to the formation of micro-joints between the pin and the disc. As a consequence of their relative movement, the softer material breaks, leaving a small void in the Mg alloy and transferring some material to the steel disc. Fig. 10 presents some evidence of the existence of adhesion wear mechanism in the worn surface of investigated alloys. Therefore, it can be concluded that these as–cast alloys had experienced a mild abrasive oxidative wear with little adhesion, as indicated in Fig. 10.

5. Conclusions

1. The optimal Ca addition is 0.3 wt.% which can effectively modify the morphology and refine the size of the primary Mg_2Si in hypereutectic Mg–5 wt.%Si alloy.
2. Excessive Ca addition results in over-modification due to the formation of some needle-like and blocky CaMgSi particles.
3. The modification mechanism is mainly due to poisoning effect, resulting from the segregation of Ca atoms at the growth front of the Mg_2Si and the adsorption effect of some of Ca atoms in the Mg_2Si crystal growth plane.
4. The addition of Ca improves the hardness of hypereutectic Mg–5 wt.%Si alloy. The optimal hardness can be achieved with Ca addition of 0.3 wt.%.
5. The prepared hypereutectic Mg–5 wt.%Si alloy with addition of 0.3 wt.%Ca has the best wear resistance among all the other alloys due to the lowest weight loss. The high weight loss of the alloys with Ca additions of 0.6 wt.% or 1 wt.% is mainly attributed to the presence of needle-like CaMgSi particles.
6. The wear mechanism of investigated alloys is a mild abrasive oxidative wear with little adhesion.

Acknowledgment

The authors would like to appreciate the financial support from Academy of Scientific Research and Technology in the framework of the scholarship for support of Ph.D. study, Egypt.

References

[1] Q. Yang, B. Jiang, X. Li, H. Dong, W. Liu, F. Pan, J. Magn. Alloys 2 (2014) 8.
[2] D. Wang, J. Zhang, J. Xu, Z. Zhao, W. Cheng, C. Xu, J. Magn. Alloys 2 (2014) 78.
[3] S.V. Muley, S.P. Singh, P. Sinha, P.P. Bhingole, G.P. Chaudhari, Mater. Des. 53 (2014) 475.
[4] J. Zhang, W. Li, Z. Guo, J. Magn. Alloys 1 (2013) 31.
[5] Z. Huanga, S. Yu, J. Alloys Compd. 546 (2013) 28.
[6] M.B. Yang, J. Zhang, T.Z. Guo, Mater. Des. 52 (2013) 274.
[7] F. Mirshahi, M. Meratian, Mater. Des. 33 (2012) 557.
[8] H.Y. Wang, L. Chen, B. Liu, X.R. Li, J.G. Wang, Q.C. Jiang, Mater. Chem. Phys. 135 (2012) 358.
[9] H.Y. Wang, M. Zha, B. Liu, D.M. Wang, Q.C. Jiang, J. Alloys Compd. 480 (2009) L25.
[10] G.R. Ma, X.L. Li, L. Li, X. Wang, Q.F. Li, Mater. Charact. 62 (2011) 360.
[11] M.E. Moussa, M.A. Waly, A.M. El-Sheikh, J. Alloys Compd. 577 (2013) 693.
[12] K.K.A. Kumar, U.T.S. Pillai, B.C. Pai, M. Chakraborty, Wear 303 (2013) 56.
[13] Q.C. Jiang, H.Y. Wang, Y. Wang, B.X. Ma, J.G. Wang, Mater. Sci. Eng. A 392 (2005) 130.
[14] K. Kondoh, H. Oginuma, R. Tuzuki, T. Aizawa, Mater. Trans. 44 (2003) 611.
[15] L.X. Lin, C.Y. Bin, W. Xiang, M.G. Rui, Trans. Nonferrous Met. Soc. China 20 (2010) s393.
[16] L. Lu, K.K. Thong, M. Gupta, Compos. Sci. Technol. 63 (2003) 627.
[17] N. Zheng, H.Y. Wang, Z.H. Gu, W. Wang, Q.C. Jiang, J. Alloys Compd. 463 (2008) L1.
[18] H.Y. Wang, W. Wang, M. Zha, N. Zheng, Z.H. Gu, D. Li, Q.C. Jiang, Mater. Chem. Phys. 108 (2008) 353.
[19] L.P. Wang, E.J. Guo, B.X. Ma, J. Rare Earths 26 (2008) 105.
[20] N. Zheng, H.Y. Wang, F. Zhao, Z.H. Gu, D. Li, Q.C. Jiang, Trans. Nonferrous Met. Soc. China 17 (2007) s440.
[21] M.Q. Cong, Z.Q. Li, J.S. Liu, S. Li, Mater. Des. 53 (2014) 430.
[22] T.S. Giu, Z.J. Xue, T.C. Wen, Y.Y. Sheng, Trans. Nonferrous Met. Soc. China 21 (2011) 1932.
[23] M.Q. Cong, Z.Q. Li, J.S. Liu, M.Y. Yan, K. Chen, Y.D. Sun, M. Huang, C. Wang, B. Ding, S. Wang, J. Alloys Compd. 539 (2012) 168.
[24] G.Y. Yuan, M.P. Liu, W.J. Ding, A. Inoue, Mater. Sci. Eng. A 357 (2003) 314.
[25] G.Y. Yuan, Z.L. Liu, Q.D. Wang, W.J. Ding, Mater. Lett. 56 (2002) 53.
[26] J. Hou, C. Li, X. Liu, J. Alloys Compd. 509 (2011) 735.
[27] K. Chen, Z.Q. Li, J.S. Liu, J.N. Yang, Y.D. Sun, S.G. Bian, J. Alloys Compd. 487 (2009) 293.
[28] E.J. Guo, B.X. Ma, L.P. Wang, J. Mater. Process. Technol. 206 (2008) 161.
[29] G.F.V. Voort, Metallography and Microstructures, first ed., ASM Handbook, USA, 2004.
[30] X. Liu, Y. Osawa, S. Takamori, T. Mukai, Mater. Sci. Eng. A 487 (2008) 120.
[31] M.B. Yang, F.S. Pan, R. Cheng, J. Shen, Mater. Sci. Eng. A 489 (2008) 413.
[32] K.M. Asl, A. Masoudi, F. Khomamizadeh, Mater. Sci. Eng. A 527 (2010) 2027.
[33] A.S. Anasyida, A.R. Daud, M.J. Ghazali, Mater. Des. 31 (2010) 365.
[34] N.N. Aung, W. Zhou, L.E.N. Lim, Wear 265 (2008) 780.
[35] C. Taltalvull, B. Torres, A.J. López, J. Rams, Mater. Des. 56 (2014) 549.